

Supporting Information

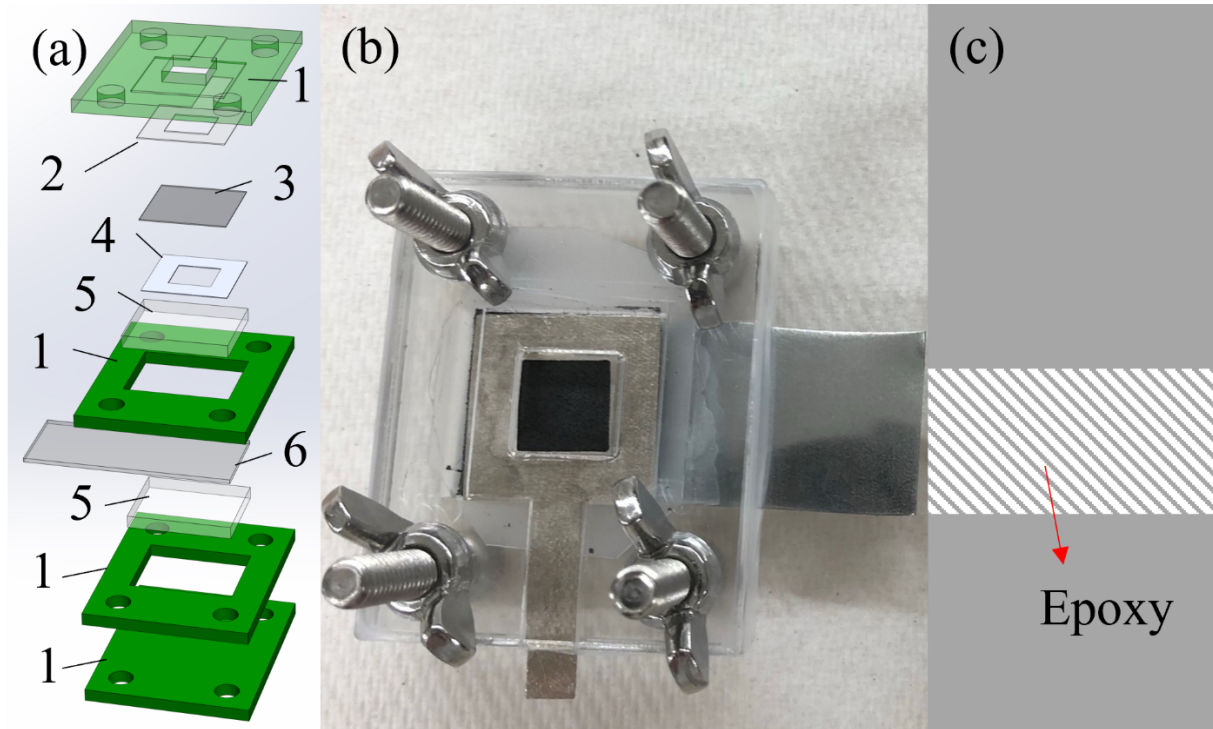


Figure S1. (a) Schematic of the sandwich-type cell in a disassembled view. (b) Optical image of the sandwich-type cell in an assembled view. (c) Illustration of Zn foil coated with epoxy. Note that the numbers correspond to the following: 1) Acrylic sheets, 2) Ni current collector, 3) GDL or carbon cloth coated with electrocatalyst, 4) polypropylene film, 5) GPE, and 6) Zn foil.

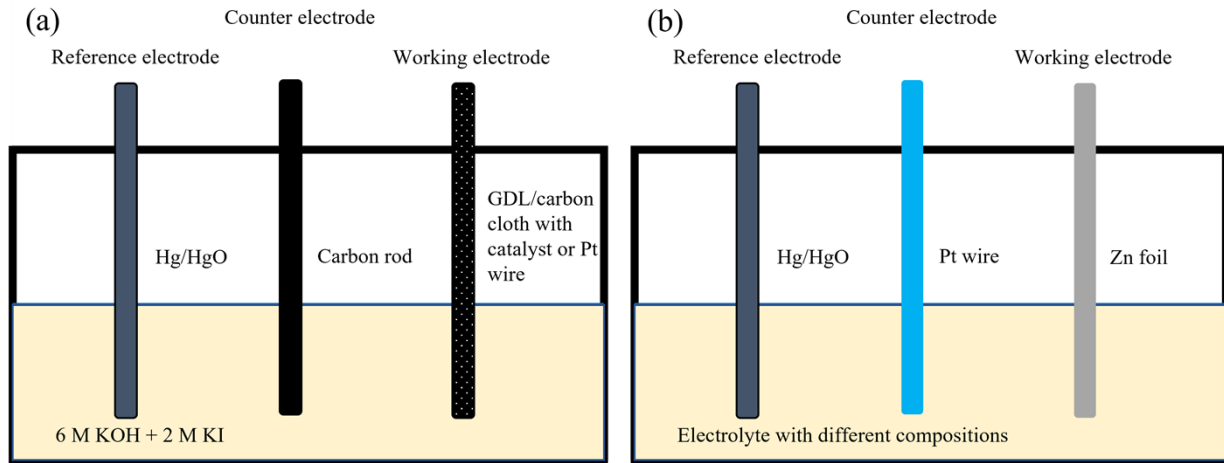


Figure S2. (a) Three-electrode setup for CV tests at the air electrode. (b) Three-electrode setup for CV tests at the Zn electrode.

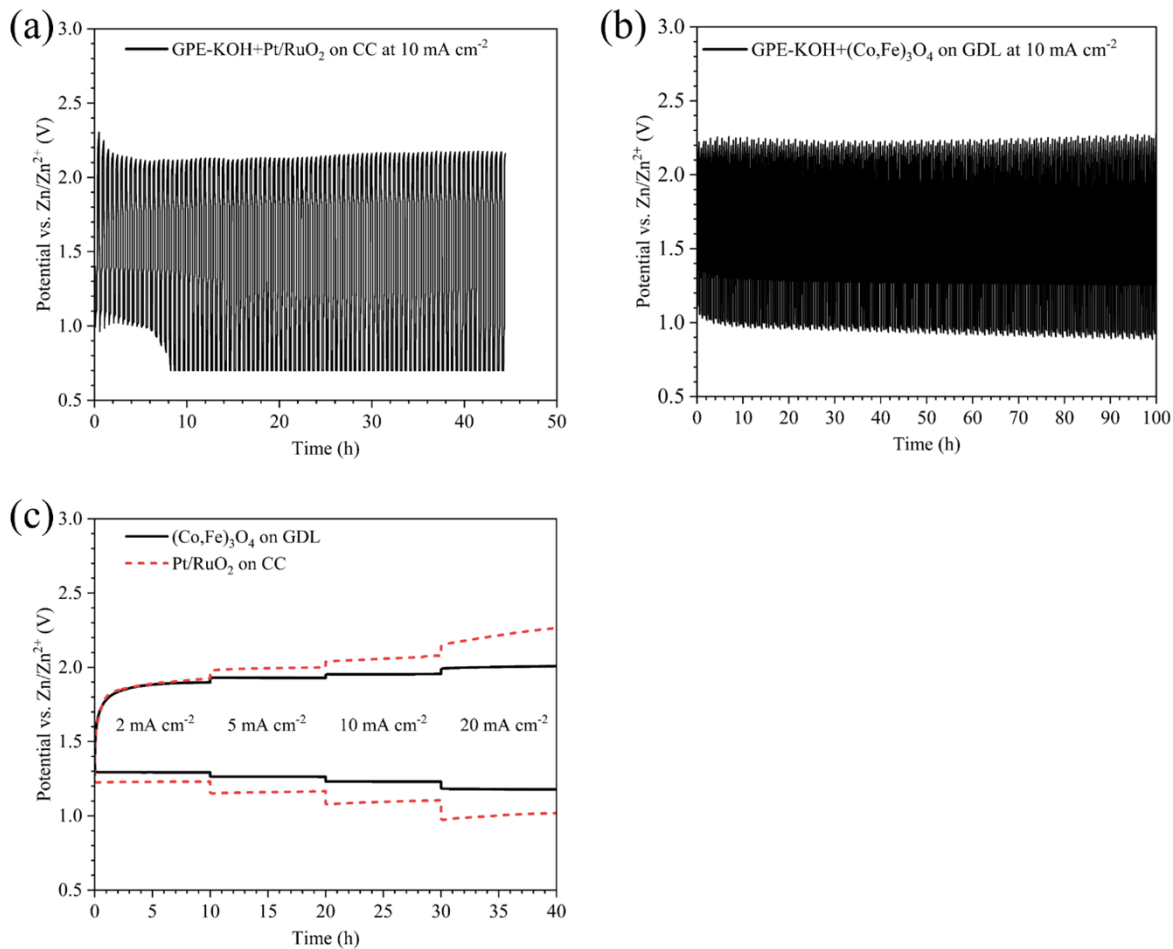


Figure S3. (a) Cyclability test at 21°C and 10 mA cm⁻² for ZAB using GPE-KOH and Pt/RuO₂ coated CC as the air electrode. (b) Cyclability test at 21°C and 10 mA cm⁻² for ZAB using GPE-KOH and (Co,Fe)₃O₄ coated GDL. (c) Rate test results for ZABs using GPE-KOH with (Co,Fe)₃O₄ on GDL and Pt/RuO₂ on CC as the air electrode at 21°C.

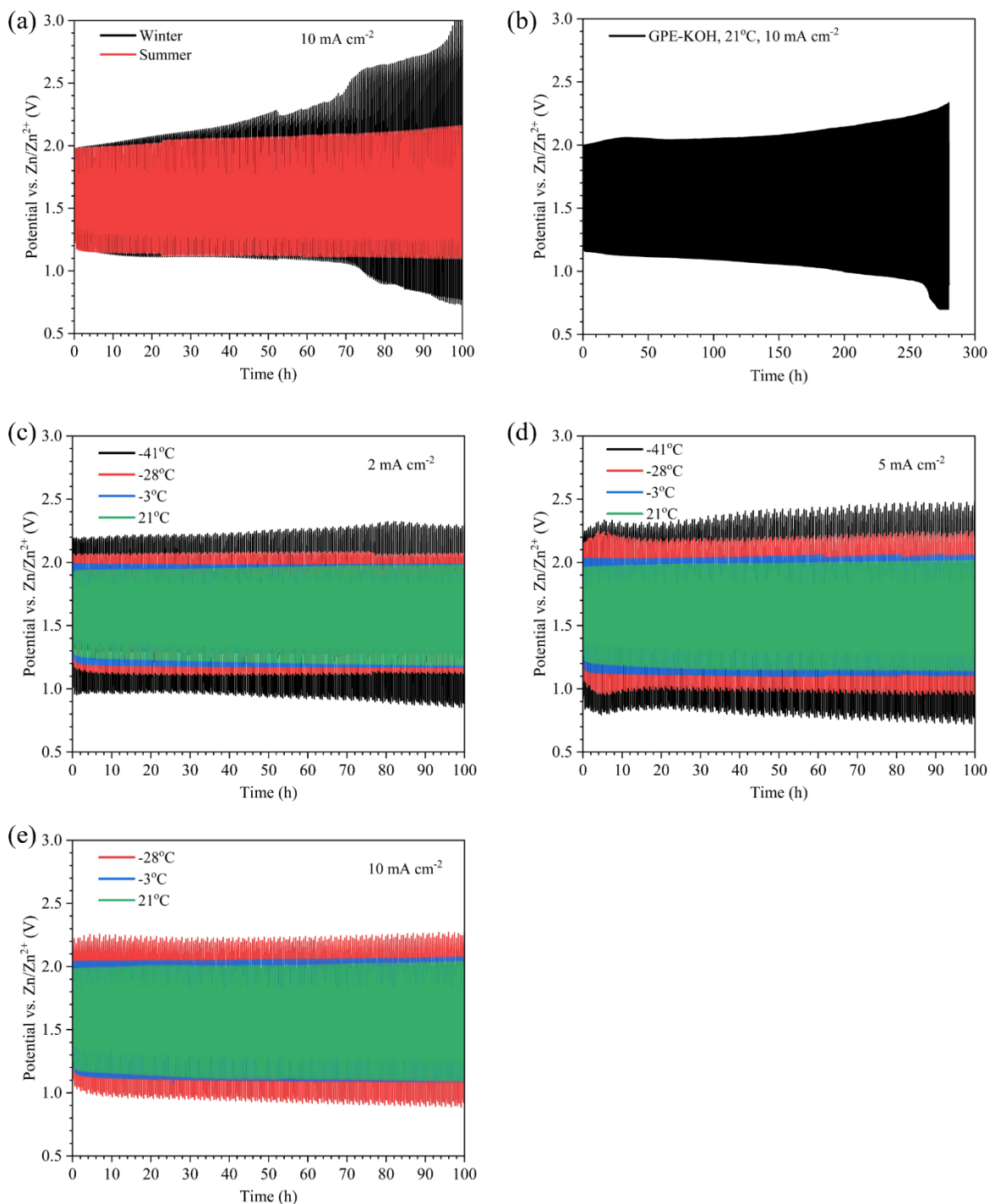


Figure S4. (a) Cyclability test at 21°C and 10 mA cm⁻² for ZAB using GPE-KOH in different seasons. (b) Full view of the lifetime test for ZAB using GPE-KOH. (c) Cyclability tests at different temperatures for ZABs using GPE-KOH and (Co,Fe)₃O₄ coated GDL at (c) 2 mA cm⁻², (d) 5 mA cm⁻², (e) 10 mA cm⁻².

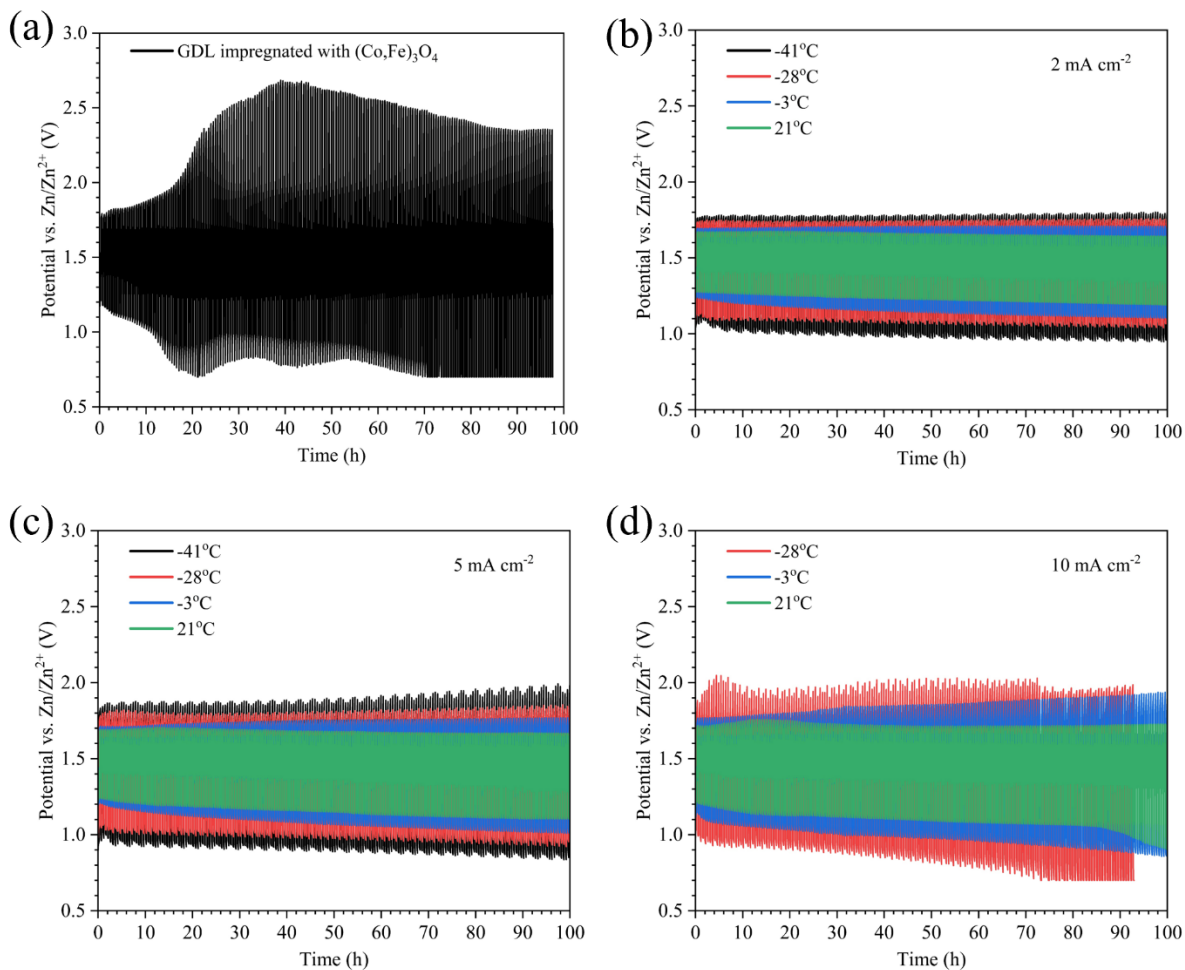


Figure S5. (a) Cyclability test at 10 mA cm^{-2} using aqueous $6 \text{ M KOH} + 2 \text{ M KI} + 0.4 \text{ M ZnO}$ as the electrolyte and GDL with $(\text{Co},\text{Fe})_3\text{O}_4$ decorated N-CNTs as the air electrode. Cyclability tests at different temperatures for ZABs using GPE-KOH-KI and Pt/RuO₂ coated CC at (b) 2 mA cm^{-2} , (c) 5 mA cm^{-2} , and (d) 10 mA cm^{-2} .

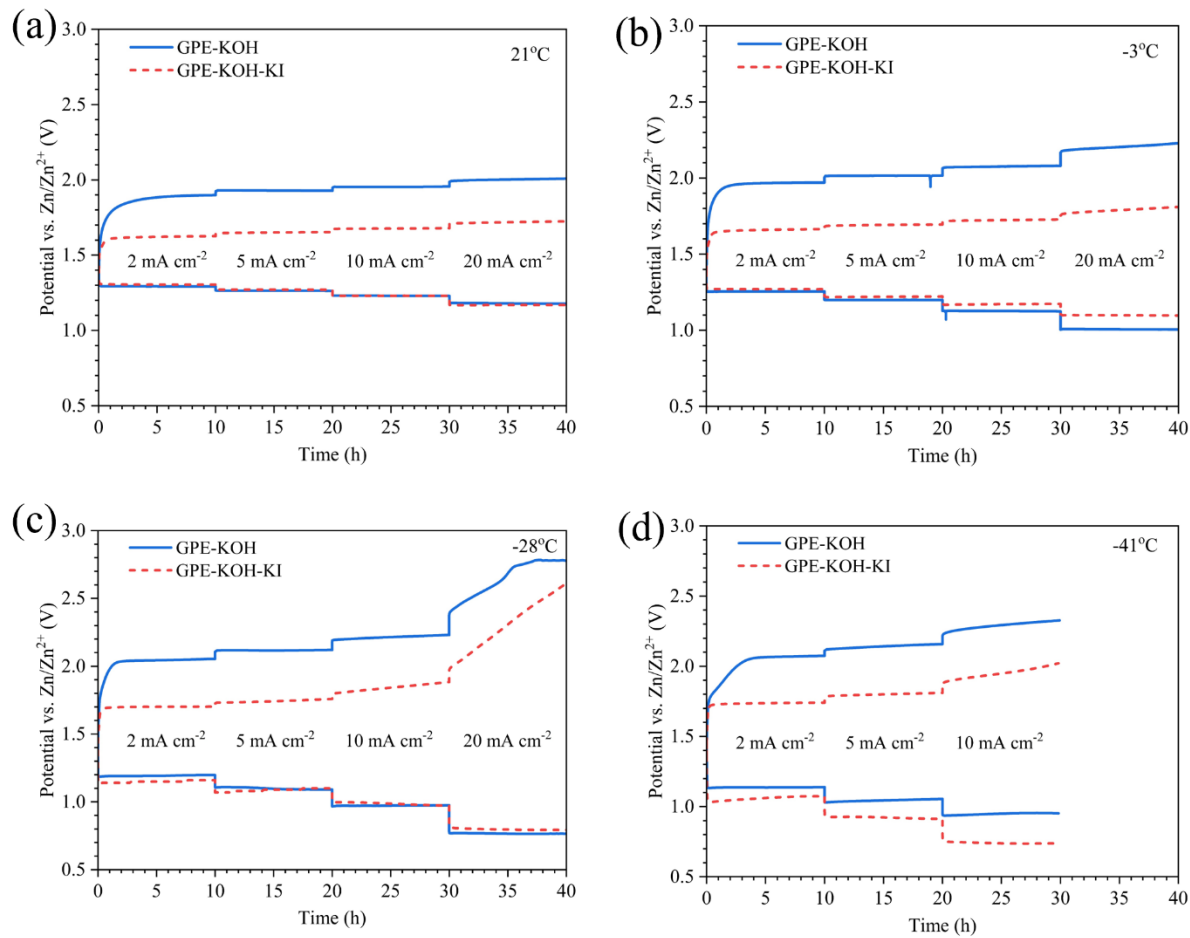


Figure S6. Comparison of rate test results for ZABs using $(\text{Co},\text{Fe})_3\text{O}_4$ coated GDL with GPE-KOH and Pt/RuO₂ coated CC with GPE-KOH-KI at (a) 21°C, (b) -3°C, (c) -28°C, and (d) -41°C.

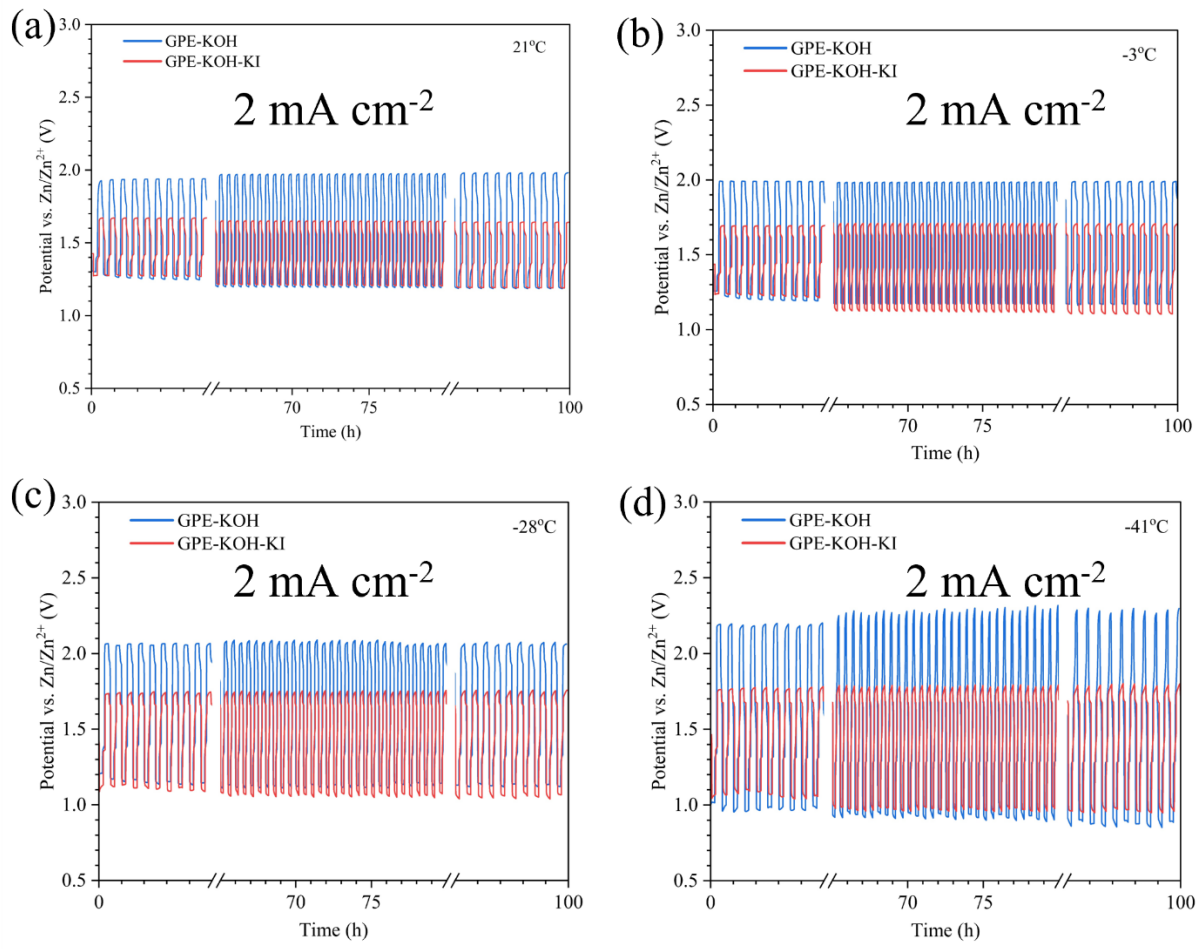


Figure S7. Cyclability test results for ZABs using $(\text{Co}, \text{Fe})_3\text{O}_4$ coated GDL with GPE-KOH and Pt/RuO₂ coated CC with GPE-KOH-KI at 2 mA cm^{-2} at (a) 21°C , (b) -3°C , (c) -28°C , and (d) -41°C .

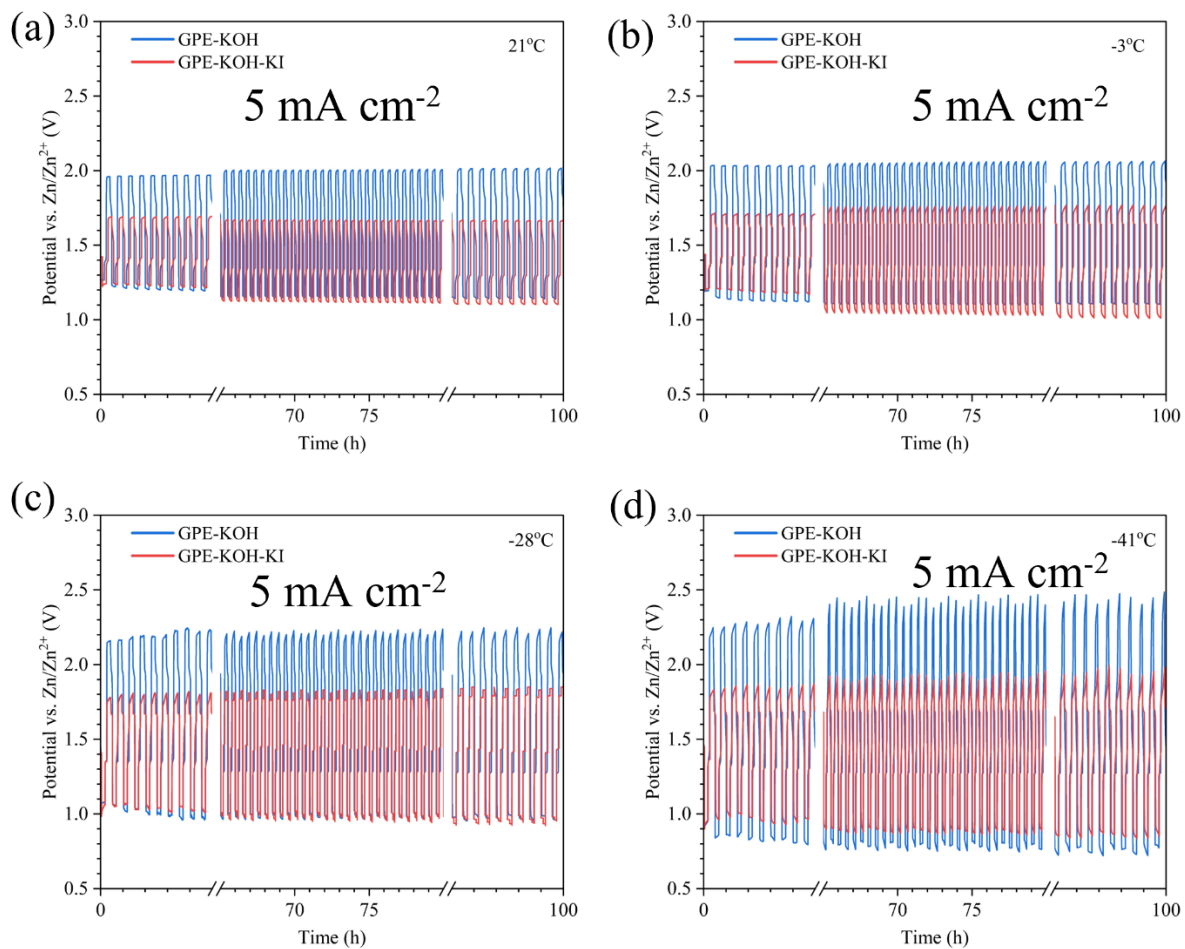


Figure S8. Comparison of cyclability test results for ZABs using $(\text{Co},\text{Fe})_3\text{O}_4$ coated GDL with GPE-KOH and Pt/RuO₂ coated CC with GPE-KOH-KI at 5 mA cm^{-2} at (a) 21°C , (b) -3°C , (c) -28°C , and (d) -41°C .

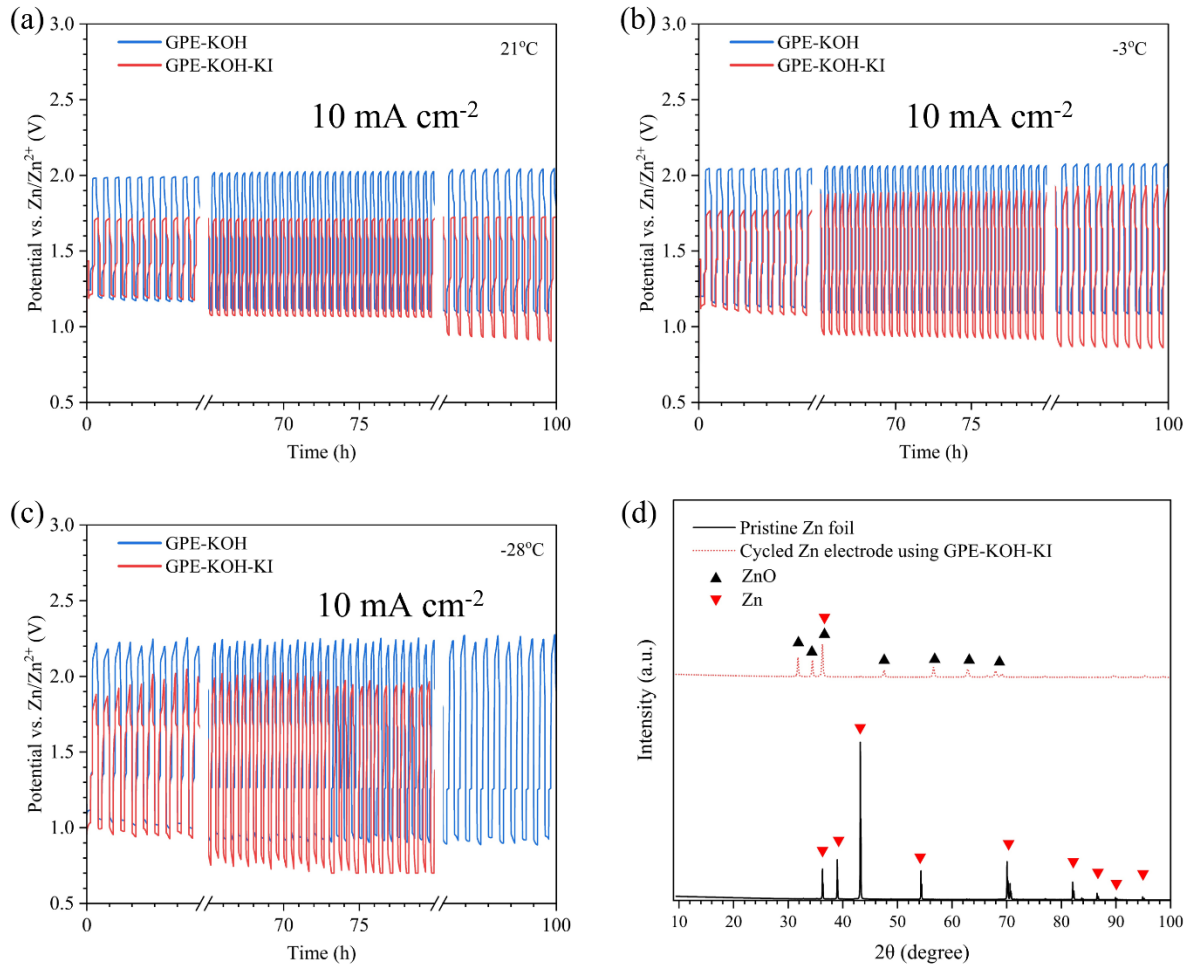


Figure S9. Cyclability test results for ZABs using $(Co,Fe)_3O_4$ coated GDL with GPE-KOH and Pt/RuO₂ coated CC with GPE-KOH-KI at 10 mA cm^{-2} at (a) $21^{\circ}C$, (b) $-3^{\circ}C$, and (c) $-28^{\circ}C$. (d) XRD patterns for pristine Zn foil and the Zn electrode after cycling using GPE-KOH-KI at $21^{\circ}C$ and 10 mA cm^{-2} for 100 h.

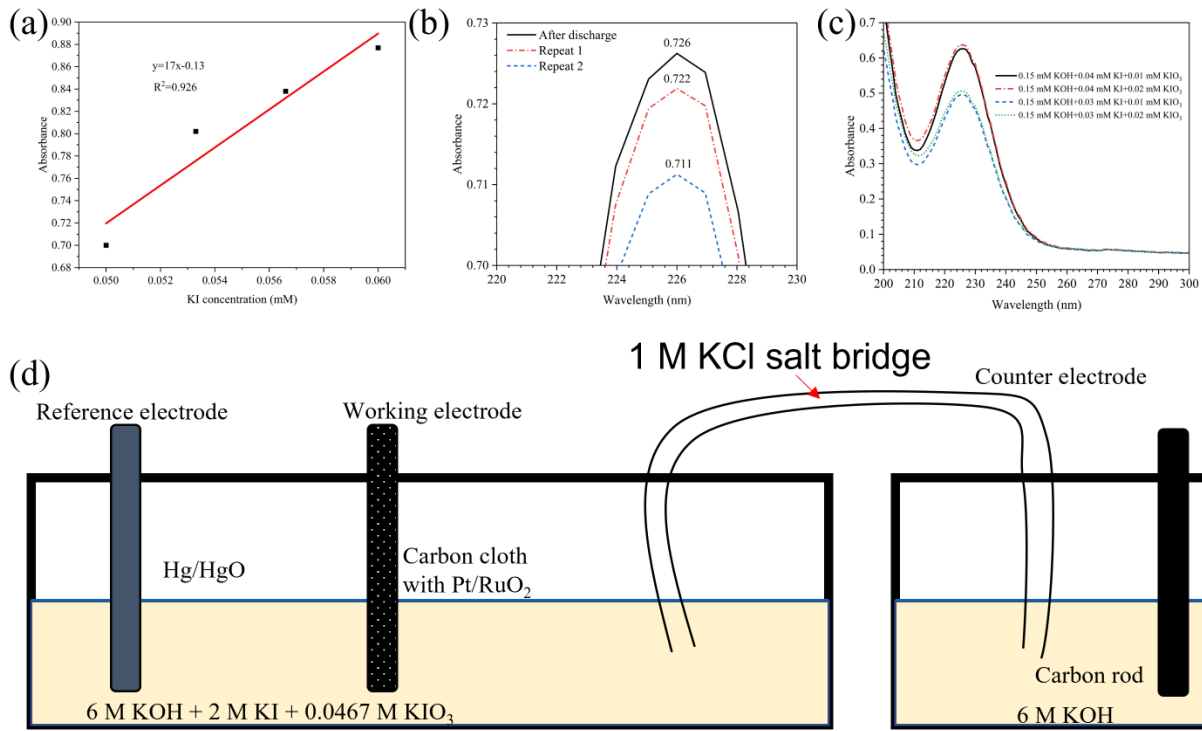


Figure S10. (a) Absorbance vs. KI concentration. This plot was created using the data in Figure 7d. UV-vis spectra for (b) sample A after discharge and with repeated diluted samples to confirm reproducibility, and (c) solutions with different concentrations of KI and KIO₃. (d) The three-electrode setup for the half-cell discharge process.

Table S1. Summary of rate test battery efficiencies and power densities for ZABs using GPE-KOH under different test conditions

Temperature (°C)	Efficiency at different current densities (%)				Peak power density (mW cm ⁻²)
	2 mA cm ⁻²	5 mA cm ⁻²	10 mA cm ⁻²	20 mA cm ⁻²	
21	68	67	63	59	127
-3	64	60	54	45	38
-28	58	51	43	27	17
-41	55	49	41	Failed	11

Table S2. Summary of cyclability test battery efficiencies for ZABs using GPE-KOH under different test conditions

Temperature (°C)	2 mA cm ⁻²		5 mA cm ⁻²		10 mA cm ⁻²	
	Initial Efficiency (%)	Final Efficiency (%)	Initial Efficiency (%)	Final Efficiency (%)	Initial Efficiency (%)	Final Efficiency (%)
21	68	60	64	57	63	53
-3	63	59	59	53	59	52
-28	58	54	50	43	50	41
-41	46	39	42	32	Failed	Failed

Table S3. Summary of rate test battery efficiencies and power densities for ZABs using GPE-KOH-KI under different test conditions

Temperature (°C)	Efficiency at different current densities (%)				Peak power density (mW cm ⁻²)
	2 mA cm ⁻²	5 mA cm ⁻²	10 mA cm ⁻²	20 mA cm ⁻²	
21	80	77	73	67	98
-3	76	72	68	61	27
-28	68	63	54	31	22
-41	61	50	37	Failed	11

Table S4. Summary of rate test battery efficiency improvement for ZABs using GPE-KOH-KI under different testing conditions when compared with ZABs using GPE-KOH

Temperature (°C)	Efficiency improvement at various current densities (%)			
	2 mA cm ⁻²	5 mA cm ⁻²	10 mA cm ⁻²	20 mA cm ⁻²
21	18	15	16	14
-3	19	20	26	36
-28	17	24	26	15
-41	11	2	-10	Both failed

Table S5. Summary of cyclability test battery efficiencies for ZABs using GPE-KOH-KI under different test conditions

Temperature (°C)	2 mA cm ⁻²		5 mA cm ⁻²		10 mA cm ⁻²	
	Initial Efficiency (%)	Final Efficiency (%)	Initial Efficiency (%)	Final Efficiency (%)	Initial Efficiency (%)	Final Efficiency (%)
21	77	73	74	66	71	52
-3	73	65	71	57	65	45
-28	65	61	60	52	55	Failed
-41	61	53	52	43	Failed	Failed

Table S6. Summary of cyclability test initial and final battery efficiency improvements for ZABs using GPE-KOH-KI under different test conditions when compared with ZABs using GPE-KOH

Temperature (°C)	2 mA cm ⁻²		5 mA cm ⁻²		10 mA cm ⁻²	
	Initial Efficiency (%)	Final Efficiency (%)	Initial Efficiency (%)	Final Efficiency (%)	Initial Efficiency (%)	Final Efficiency (%)
21	13	22	16	16	13	-2
-3	16	10	20	8	10	-13
-28	12	13	20	21	10	None
-41	33	36	24	34	N/A	N/A

Table S7. Comparison of ZABs using GPEs reported in this work and in the literature

Electrolyte	Current Density (mA cm ⁻²)	Temp. (°C)	Catalyst	Maximum Power Density (mW cm ⁻²)	Initial Battery Efficiency (%)	Cycling Time (h)	Ref.		
GPE-KOH	2	21	(Co,Fe) ₃ O ₄	127	68	100	This work		
		-28		17	58	100			
		-41		11	46	100			
	10	21		127	61	260			
	2	21	Pt/RuO ₂	98	77	100			
GPE-KOH-KI		-28		22	65				
		-41		11	61				
		5		98	77				
		21		98	77				
PAM-PAA	1	25	Pt/RuO ₂	11.8	66	10	1		
		-20		8.2	55	10			
Cellulose-PAA	2	25	MnO ₂ , Co ₃ O ₄	40.25	69	11	2		
PAM	5	25	MnO ₂ , GO	105	63	23.3	3		
PVA	3	25	Co ₃ O ₄	62.6	63	48	4		
PAA	2	25	FeCo based catalyst	160	65	105	5		
	5	25			~60	80			
	2	-20		80.5	57	5			
PAMPS-K/MC	1	25	Co ₃ O ₄	73.9	64	24	6		
		0		N/A	~60				
		-20		54.2	~55				
PAM-KI	2	20	Pt/RuO ₂	43	71	75	7		
		-40		10	59	40			
PANa-starch	1	25	Pt/RuO ₂	67.5	68	28.7	8		
		-20		30.7	~53	44.1			
PAA	2	25	FeCo based catalyst	128.8	65.9	92	9		
		-30		63.6	60.4	92			
PANa	2	25	Pt/RuO ₂	88	65.5	160	10		
PANa-cellulose	5	25	Fe based	108.6	60	110	11		
PVA-GG	2	25	Pt/IrO ₂	50	~60	10	12		
PVA	1	25	Co ₃ O ₄	N/A	~38	70	13		
PVA	1	25	Co ₃ O ₄	16	~39	40	14		
PVA-PAA-GO-KI	2	25	Pt/C+Co ₃ O ₄	78.6	73	200	15		
Aqueous 6 M KOH+3 M KI+0.2 M Zn(Ac) ₂	5	25	Pt/C	148.8	76.5	80	16		
PEVA	2	25	Co ₃ O ₄	N/A	~60	230	17		
PAM-SA-KI	1	25	PtC/RuO ₂	132	80	110	18		

Abbreviations:

PAMPS-K/MC: poly(2-acrylamido-2-methylpropanesulfonic acid potassium salt) with methyl cellulose

PANa-starch: sodium polyacrylate-starch

GG: guar hydroxypropyltrimonium chloride

GO: graphene oxide

SA: sodium alginate

PEVA: poly(ethylene vinyl acetate)

Table S8. Summary of rate test battery efficiencies and power densities for ZABs using GPE-KOH and GPE-KOH-KI under different conditions

GPE-KOH					
Temperature (°C)	2 mA cm⁻²	5 mA cm⁻²	10 mA cm⁻²	20 mA cm⁻²	Peak power density (mW cm⁻²)
21	68	67	63	59	127
-3	64	60	54	45	38
-28	58	51	43	27	17
-41	55	49	41	Failed	11
GPE-KOH-KI					
Temperature (°C)	2 mA cm⁻²	5 mA cm⁻²	10 mA cm⁻²	20 mA cm⁻²	Peak power density (mW cm⁻²)
21	80	77	73	67	98
-3	76	72	68	61	27
-28	68	63	54	31	22
-41	61	50	37	Failed	11

Table S9. Summary of cyclability performance of ZABs using GPE-KOH and GPE-KOH-KI under different conditions

GPE-KOH						
	2 mA cm ⁻²		5 mA cm ⁻²		10 mA cm ⁻²	
Temperature (°C)	Initial Efficiency (%)	Final Efficiency (%)	Initial Efficiency (%)	Final Efficiency (%)	Initial Efficiency (%)	Final Efficiency (%)
21	68	60	64	57	63	53
-3	63	59	59	53	59	52
-28	58	54	50	43	50	41
-41	46	39	42	32	Failed	Failed
GPE-KOH-KI						
	2 mA cm ⁻²		5 mA cm ⁻²		10 mA cm ⁻²	
Temperature (°C)	Initial Efficiency (%)	Final Efficiency (%)	Initial Efficiency (%)	Final Efficiency (%)	Initial Efficiency (%)	Final Efficiency (%)
21	77	73	74	66	71	52
-3	73	65	71	57	65	45
-28	65	61	60	52	55	Failed
-41	61	53	52	43	Failed	Failed

Table S10. Ionic mobility of selected ions in water

Ion	Mobility ($10^{-8} \text{ m}^2 \text{ s}^{-1} \text{ V}^{-1}$)	Reference
K ⁺	7.62	19
OH ⁻	20.64	19
I ⁻	6.23±0.04	20

References

- 1 R. Chen, X. Xu, S. Peng, J. Chen, D. Yu, C. Xiao, Y. Li, Y. Chen, X. Hu, M. Liu, H. Yang, I. Wyman and X. Wu, *ACS Sustain. Chem. Eng.*, 2020, **8**, 11501–11511.
- 2 G. Zhang, X. Cai, C. Li, J. Yao, Z. Tian, F. Zhang, Y. Liu, W. Liu and X. Zhang, *Int. J. Biol. Macromol.*, 2022, **221**, 446–455.
- 3 H. Miao, B. Chen, S. Li, X. Wu, Q. Wang, C. Zhang, Z. Sun and H. Li, *J. Power Sources*, 2020, **450**, 227653.
- 4 X. Fan, J. Liu, Z. Song, X. Han, Y. Deng, C. Zhong and W. Hu, *Nano Energy*, 2019, **56**, 454–462.
- 5 Z. Pei, Z. Yuan, C. Wang, S. Zhao, J. Fei, L. Wei, J. Chen, C. Wang, R. Qi, Z. Liu and Y. Chen, *Angew. Chemie - Int. Ed.*, 2020, **59**, 4793–4799.
- 6 N. Sun, F. Lu, Y. Yu, L. Su, X. Gao and L. Zheng, *ACS Appl. Mater. Interfaces*, 2020, **12**, 11778–11788.
- 7 Y. Zhang, H. Qin, M. Alfred, H. Ke, Y. Cai, Q. Wang, F. Huang, B. Liu, P. Lv and Q. Wei, *Energy Storage Mater.*, 2021, **42**, 88–96.
- 8 Y. Zhang, Y. Chen, M. Alfred, F. Huang, S. Liao, D. Chen, D. Li and Q. Wei, *Compos. Part B Eng.*, 2021, **224**, 109228.
- 9 Z. Pei, L. Ding, C. Wang, Q. Meng, Z. Yuan, Z. Zhou, S. Zhao and Y. Chen, *Energy Environ. Sci.*, 2021, **14**, 4926–4935.
- 10 Y. Huang, Z. Li, Z. Pei, Z. Liu, H. Li, M. Zhu, J. Fan, Q. Dai, M. Zhang, L. Dai and C. Zhi, *Adv. Energy Mater.*, 2018, **8**, 1802288.
- 11 L. Ma, S. Chen, D. Wang, Q. Yang, F. Mo, G. Liang, N. Li, H. Zhang, J. A. Zapien and C. Zhi, *Adv. Energy Mater.*, 2019, **9**, 1803046.
- 12 M. Wang, N. Xu, J. Fu, Y. Liu and J. Qiao, *J. Mater. Chem. A*, 2019, **7**, 11257–11264.
- 13 Y. Li, X. Fan, X. Liu, S. Qu, J. Liu, J. Ding, X. Han, Y. Deng, W. Hu and C. Zhong, *J. Mater. Chem. A*, 2019, **7**, 25449–25457.
- 14 C. Lin, S. S. Shinde, X. Li, D.-H. Kim, N. Li, Y. Sun, X. Song, H. Zhang, C. H. Lee, S. U. Lee and J.-H. Lee, *ChemSusChem*, 2018, **11**, 3215–3224.
- 15 Z. Song, J. Ding, B. Liu, X. Liu, X. Han, Y. Deng, W. Hu and C. Zhong, *Adv. Mater.*, 2020, **32**, 1908127.
- 16 S. Zhao, T. Liu, Y. Dai, J. Wang, Y. Wang, Z. Guo, J. Yu, I. T. Bello and M. Ni, *Appl. Catal. B Environ.*, 2023, **320**, 121992.
- 17 Z. Chen, X. Yang, W. Li, X. Liang, J. Guo, H. Li, Y. He and Y. Kim, *Small*, 2021, **17**, 2103048.
- 18 Q. Liu, C. Xia, C. He, W. Guo, Z. P. Wu, Z. Li, Q. Zhao and B. Y. Xia, *Angew. Chemie Int. Ed.*, 2022, **134**, e202210567.

- 19 J. R. Varcoe, P. Atanassov, D. R. Dekel, A. M. Herring, M. A. Hickner, P. A. Kohl, A. R. Kucernak, W. E. Mustain, K. Nijmeijer, K. Scott, T. Xu and L. Zhuang, *Energy Environ. Sci.*, 2014, **7**, 3135–3191.
- 20 S. Koneshan, J. C. Rasaiah, R. M. Lynden-Bell and S. H. Lee, *J. Phys. Chem. B*, 1998, **102**, 4193–4204.